International Journal of Production Research

ISSN: 0020-7543 (Print) 1366-588X (Online) Journal homepage: https://www.tandfonline.com/loi/tprs20

Travel time model for double-deep shuttle-based storage and retrieval systems

Tone Lerher

To cite this article: Tone Lerher (2016) Travel time model for double-deep shuttle-based storage and retrieval systems, International Journal of Production Research, 54:9, 2519-2540, DOI: 10.1080/00207543.2015.1061717

To link to this article: https://doi.org/10.1080/00207543.2015.1061717

International Journal of Production Research, 2016
Vol. 54, No. 9, 2519–2540, http://dx.doi.org/10.1080/00207543.2015.1061717

Taylor & Francis
Taylor & Francis Group

Travel time model for double-deep shuttle-based storage and retrieval systems

Tone Lerher*

Faculty of Mechanical Engineering, University of Maribor, Maribor, Slovenia

(*Received 20 December 2014; accepted 4 June 2015*)

Technological developments in the global supply chain have changed processes in warehousing. This reflects in short response time in handling the orders, which has a consequence on high automation degree in warehousing. An important part of automated warehouses is presented by shuttle-based storage and retrieval systems (SBS/RS), which are used in practice when demand for the throughput capacity is high. In this paper, analytical travel time model for the computation of cycle times for double-deep SBS/RS is presented. The advantage of the double-deep SBS/RS is that fewer aisles are needed, which results in a more efficient use of floor space. The proposed model considers the real operating characteristics of the elevators lifting table and the shuttle carrier with the condition of rearranging blocking totes to the nearest free storage location during the retrieval process of the shuttle carrier. Assuming uniform distributed storage locations and the probability theory, the expressions for the single and dual-command cycle of the elevators lifting table and the shuttle carrier have been determined. The proposed model enables the calculation of the expected cycle time for single- and dual-command cycles, from which the performance of the double-deep SBS/RS can be evaluated. The analysis show that regarding examined type of the double-deep SBS/RS, the results of the proposed analytical travel time model demonstrate good performances for evaluating double-deep SBS/RS.

Keywords: Automated warehouses; Double-deep system; Shuttle-based storage and retrieval systems; Analytical modelling, performance analysis

1. Introduction

Warehouses are important part in the global supply chain. With regards to the rapid development of automated material handling equipment, new designs of automated warehouses have been developed.

An important part of automated warehouses is represented by shuttle-based storage and retrieval systems (SBS/RS). The basic components of SBS/RS are storage racks (SR), an elevator with the lifting table for feeding the SBS/RS with totes, shuttle carriers, which are operating in each tier (tier-captive system), buffer positions at each tier, input/output (I/O) location and accumulating conveyors (AC).

SBS/RS enable high-throughput capacity vs. mini-load automated storage and retrieval systems (AS/RS). Compared to mini-load AS/RS, the capital and maintenance costs of SBS/RS are relatively high. For this reason, the application of SBS/RS must be economically justifiable.

Various designs and configurations of small parts (totes) mini-load AS/RS have been made due to different market requirements. Some mini-load AS/RS have a double-deep SR. The double-deep SR is a single-deep SR that is two totes positions deep. The advantage of the double-deep SR is that fewer aisles are needed which results in a more efficient use of floor space. In most cases, a 50% aisle space saving is achieved vs. single-deep SR. Since totes are stored in the first and in the second lane of the SBS/RS, a special policy for rearranging blocking totes by a shuttle carrier to the nearest (free) storage location is needed.

The majority of current research is based on the single-deep SR only. The observation stands for the mini-load AS/RS and for the SBS/RS. Since many producers of the warehouse equipment like Dematic, Knapp, Schaefer, Stoecklin and Savoye have begun to offer double-deep and deep-lane systems in practice, there is a clear necessity to study double-deep systems. The latter was a motivation for the proposed research work.

The application of the single- or double-deep systems depends on the required warehouse volume, throughput capacity and desired level of flexibility. If there is a demand for a high warehouse volume and relatively small layout of the SR, the double-deep system would be considered as a best choice. This decision will have an impact on the throughput capacity, since the overall cycle time will be higher compared to single-deep system. This will further influence on the desired level of flexibility, since during the storage and/or retrieval process, a rearrangement of the blocking tote could happen.

*Email: tone.lerher@um.si

According to the above mentioned, the double-deep system is worthy of in-depth research to evaluate the overall system performance of relatively complex system (combining factors like warehouse volume, throughput capacity and desired level of flexibility).

The most related paper to the studied system of SBS/RS is completed by Carlo and Vis (2012). They study a type of SBS/RS where there are two non-passing lifting systems mounted along the rack.

Smew, Young, and Geraghty (2013) presented a simulation study to trade-off between the conflicting objectives of maximising customer service level and minimising work-in-process. Bekker (2013) proposed as a computationally economic approach to optimise throughout rate and allocated buffer space, which are the two conflicting objectives of the buffer allocation problem.

Marchet et al. (2013) studied the main design trade-offs for AVS/RS using simulation. They complete their study of several warehouse design scenarios for two types of AVS/RS configurations: tier-captive and tier-to-tier vehicles.

Recently, Lerher (2013) studied energy regeneration and energy efficiency models for SBS/RS. The proposed model enables reduction of energy consumption and consequently the CO_2 emission, which is vital from economic and environmental point of view.

Sari et al. (2014) studied experimental validation of travel time models for shuttle-based AS/RS.

Lerher et al. (2015a) proposed analytical travel time model for the computation of travel (cycle) time for SBS/RS. The proposed model considers the operating characteristics of the elevators lifting table and the shuttle carrier, such as acceleration and deceleration and the maximum velocity. The proposed model enables the calculation of the expected travel (cycle) time for the single- and dual-command cycles, from which the performance of SBS/RS can be evaluated.

Studies of double-deep AS/RS have been presented by Oser and Garlock (1998), Oser and Ritonja (2004) and Ritonja (2003). Studies of multi-deep AS/RS have been presented by Sari, Saygin, and Ghouali (2005). In their research, they presented travel time models for the 3D flow-rack AS/RS. De Koster, Le-Duc, and Yu (2008) presented an optimal storage rack design for the 3D-compact AS/RS. They introduced the combination of the S/R machine for transport unit load (TUL) movement in the horizontal and vertical directions and the system of inbound and outbound conveyors (powered or non-powered) for the depth movement. In the continuation of their work, Yu and De Koster (2009a) derived the expected single-command cycle time under the full turnover-based storage policy. In order to implement the class-based policy, Yu and De Koster (2009b) introduced the model for determining the optimal storage zone boundaries for the 3D compact AS/RS.

Lerher, Sraml et al. (2010) studied double-deep system for unit-load AS/RS. The proposed models consider the real operating characteristics of the storage and retrieval machine and the condition of rearranging blocking loads to the nearest free storage location during the retrieval process. The proposed models enable the calculation of the mean cycle time for single- and dual-command cycles, from which the performance of the double-deep AS/RS can be evaluated.

Xu et al. (2015) studied double-deep dual-shuttle AS/RS, which have the advantages of high space utilisation single-deep single-shuttle automated storage/retrieval systems. In their paper, they presented analytical models of quadruple-command cycle in order to estimate the system performance of double-deep dual-shuttle AS/RS. A significant improvement using dual-shuttle S/R machine due to single-shuttle S/R machine, has been observed.

According to the above literature review, multi-deep system and SBS/RS have not been discussed by many researchers in the research community. A lot of research has been done for single-deep system for mini- and unit-load AS/RS. Nevertheless, there are few papers for cycle time calculation of double-deep AS/RS (Oser and Garlock 1998; Ritonja 2003; Oser and Ritonja 2004; Lerher, Sraml et al. 2010; Xu et al. 2015).

Different from the existing studies, the previous SBS/RS model (Lerher et al. 2015a, 2015b; Sari et al. 2014) will be extended by implementing the analytical (continuous) travel time model for double-deep SBS/RS. The proposed model considers the real operating characteristics of the elevators lifting tables and the shuttle carrier under the condition of the rearrangement of the blocking totes by the shuttle carrier to the nearest storage location in the storage rack of the SBS/RS.

This paper is organised as follows: in the second section, the basic description of SBS/RS under the proposed study is given. In Section 3 analytical modelling of travel time is presented. In Section 4, the proposed analytical travel time model for double-deep SBS/RS to calculate the expected cycle time considering the rearrangement of blocking totes, is presented. In Section 5, the main analysis is given. Finally, the main conclusion is given in Section 6.

2. Shuttle-based storage and retrieval systems

SBS/RS consists of a storage rack for totes, with an elevator with lifting table and shuttle carriers, which are operating in each tier of the SBS/RS.

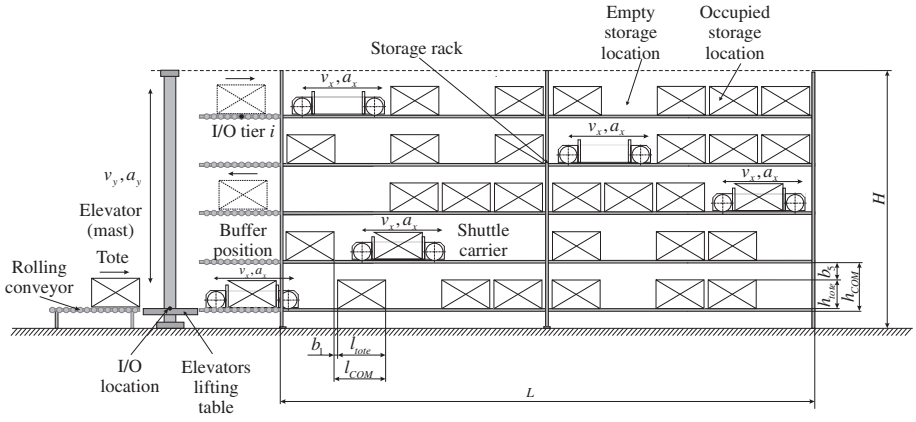

Figure 1. Typical installation of the SBS/RS.

SBS/RS of 20 m in height or more are installed in the practice. The design of SBS/RS is determined by the total amount of totes movement in a given period of time (throughput capacity of the system). Many producers of the warehouse and material handling equipment have begun to offer SBS/RS for almost 10 years. The amount of required storage locations depends on the designed warehouse (volume) capacity. The warehouse management system monitors the status of material handling components in the system (elevators lifting tables, shuttle carriers, buffer positions, etc.) and based on the order list and movement requirements, it plans the work to be carried out. The elevator consists of a vertical mast or a pair of masts supporting the lifting table (Figure 2), which are moved in the vertical direction. The elevator with its lifting table is feeding the buffer positions, which are set at the beginning of each tier of the SBS/RS. In each tier of the SR, there is a shuttle carrier that can store and retrieve totes (Lerher et al. 2015a) (Figure 1).

The installation of the SBS/RS with one lifting table works on the basis of single-command or dual-command cycle. More efficient is the application of the dual-command cycle, since the throughput capacities are higher, compared to single-command cycle. In this installation, totes arrive in the system on the right side of the SBS/RS and are departing the system on the left side of SBS/RS (Figure 2).

Since in each tier there is a single shuttle carrier, the elevator is most often the bottleneck of the SBS/RS. For this reason, newer designs of SBS/RS have installations with two lifting tables, which can work independently of each other. Thus, higher throughput capacity can be achieved (Figure 3).

The installation of the SBS/RS with two lifting tables works on the basis of single-command or dual-command cycle. In case of single-command cycle, totes arrive in the system on the right side of the SBS/RS and are departing the system on the left side of SBS/RS (Figure 3). In case of dual-command cycle, totes arrive in and depart from on the right and on the left side of the SBS/RS (Figure 3). In this case, a special management system for preventing the collision of totes on the roller conveyor is needed. As well, the special application of different tier height for totes arriving at the *i*th tier and departing at the *j*th tier is possible. More efficient is the application of the dual-command cycle, since the throughput capacities are higher compared to single-command cycle.

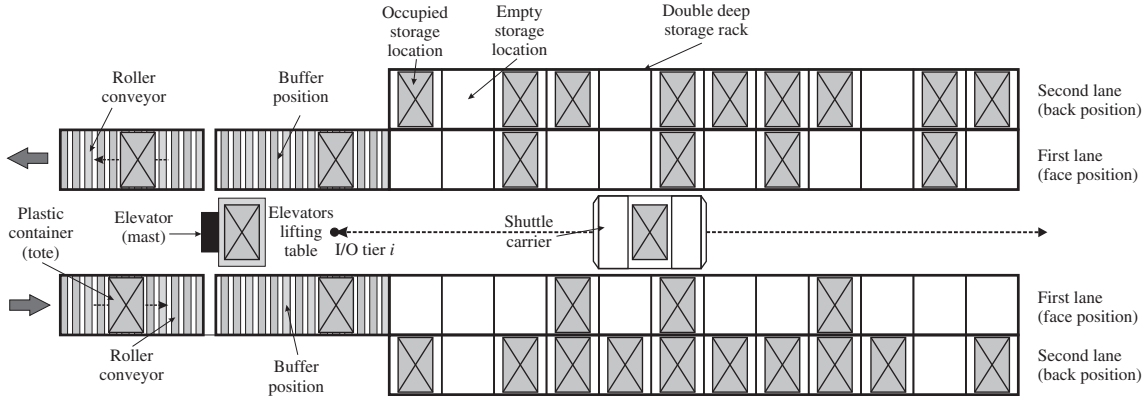

Figure 2. Installation of the SBS/RS with an elevator serving one lifting table only.

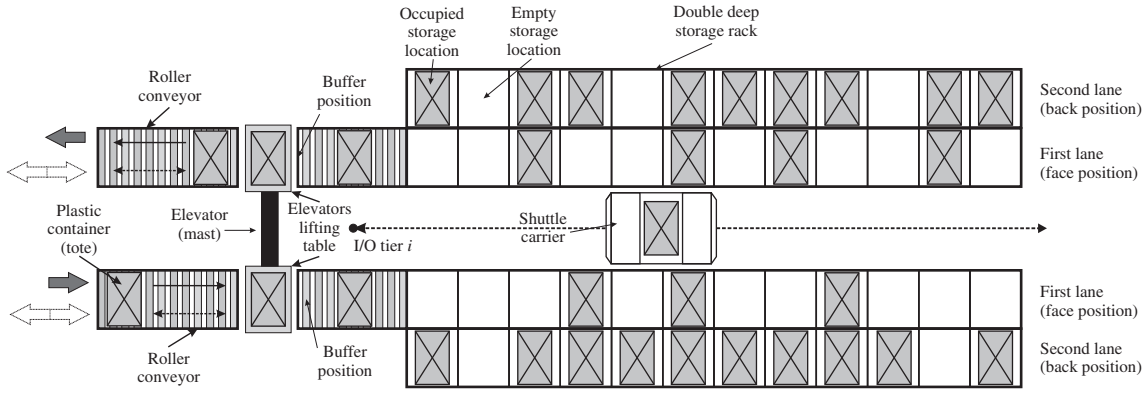

Figure 3. Installation of the SBS/RS with the elevator serving two lifting tables.

3. Analytical modelling of travel time

3.1 *Assumptions and notations*

When developing the proposed analytical travel time model for double-deep SBS/RS, the real operating characteristics of the shuttle carrier and the elevators lifting tables have been considered.

In the analysis, the following assumptions were considered:

- The double-deep SBS/RS is divided into two sides in a picking aisle. Therefore, totes can be stored in either double deep side in the *i*th tier (Figure 2).
- The I/O location of the elevator is located at the first tier (Figure 1).
- The $I/O_{tier\,i}$ location of the shuttle carrier is located at the buffer position in the *i*th tier (Figures 1 and 2).
- The dwell-point location of the shuttle carrier in the *i*th tier (when idle) is located at the $I/O_{tier\,i}$ location.
- The SR is divided by columns and tiers. At each tier, there are two buffer positions (left and right) and a single-shuttle carrier (the application of the tier-captive system, Figure 2).
- The elevator manipulates one or two lifting tables independently (Figures 1 and 2). In case of two lifting tables, one is located at the left side and the other one is located at the right side of the elevator. Each lifting table can serve one tote at a time (Figure 2).
- The elevator and the shuttle carrier operate on the basis of single- and dual-command cycles.
- The shuttle carrier has place for one tote only. In principle, but not necessary, totes will be stored first in the second lane of the SBS/RS, which will minimise the number of rearrangements during the retrieval operation.
- The shuttle carrier is equipped with the load attachments and can serve in the first and in the second lane of the SBS/RS.
- Drive characteristics (v_y, a_y) of the elevators lifting tables as well as the height H of the SR are known in advance.
- Drive characteristics of the shuttle carrier (v_x, a_x) as well as the length L of the SR are known in advance.
- The height H and length L of the SR are large enough for the elevators lifting table and the shuttle carrier to reach their maximum velocity v_{max} in the vertical and in the horizontal direction.
- Randomised assignment policy is considered, which means that any storage position is equally likely to be selected for storage or retrieval location to be processed.

The following notation is introduced:

Abbreviations

AC	Accum ulating conveyor
AVS/RS	Autonomous vehicle storage and retrieval systems
AS/RS	Automated storage and retrieval systems
CO_2	Carbon dioxide
DCC	Double-command cycle
FEM	European federation of materials handling
I/O	Input and output location

ES	One-way travel time component
P	Probability
SBS/RS	Shuttle-based storage and retrieval systems
SCC	Single-command cycle
SR	Storage rack
S/R	Storage and retrieval
3D	Three-dimensional
TB	Travel-between time component
TUL	Transport unit load

Operational parameters

a	Acceleration/deceleration
a_y	Acceleration/deceleration of the elevators lifting table
a_x	Acceleration/deceleration of the shuttle carrier
a_x^+	Acceleration of the shuttle carrier
a_y^+	Acceleration of the elevators lifting table
T	Arrival time at a destination
r_i	Closed location
$F(t)$	Cumulative distribution function
a_x^-	Deceleration of the shuttle carrier
a_y^-	Deceleration of the elevators lifting table
$s(t)$	Displacement (distance travelled) as a function of travel time
$d(T)$	Distance moved during time T
η	Efficiency
η_{LIFT}	Efficiency of the elevators lifting table
η_{SCAR}	Efficiency of the shuttle carrier
$E(R)$	Expected rearrangement cycle time
$E(t_R)$	Expected travel time from the retrieval position to the rearrangement position
$E(\mathrm{ES})_{\mathrm{SCAR}}$	Expected one-way travel time of the shuttle carrier
$E(\mathrm{SCC})_{\mathrm{SCAR}}$	Expected single-command cycle time of the shuttle carrier
$E(\mathrm{TB})_{\mathrm{SCAR}}$	Expected travel between time of the shuttle carrier
$E(\mathrm{DCC})_{\mathrm{SCAR}}$	Expected dual-command cycle time of the shuttle carrier
$E(\mathrm{ES})_{\mathrm{LIFT}}$	Expected one-way travel time of the elevators lifting table
$E(\mathrm{SCC})_{\mathrm{LIFT}}$	Expected single-command cycle time of the elevators lifting table
$E(\mathrm{TB})_{\mathrm{LIFT}}$	Expected travel between time of the elevators lifting table
$E(\mathrm{DCC})_{\mathrm{LIFT}}$	Expected dual-command cycle time of the elevators lifting table
ψ	Expected bottleneck
α	Fill-grade factor
h_{tote}	Height of the tote
h_{COM}	Height of the tier
H	Height of the storage rack
T_{kx}	Horizontal travel time depending of the regions for the travel type I and II
l_{tote}	Length of the tote
l_{COM}	Length (depth) of the column
L	Length of the storage rack
v_y	Maximum velocity of the elevators lifting table in the vertical direction
v_x	Maximum velocity of the shuttle carrier in the horizontal direction
$v_{\max}$	Maximum velocity
l	Minimum distance necessary to reach v_x
h	Minimum distance necessary to reach v_y
A	Number of aisles
C	Number of columns
n_x	Number of columns
n_{stored}	Number of stored totes

n_{total}	Number of all storage locations
M	Number of tiers
s_i	Open location
$v(t_p)$	Peak velocity at time t_p
$t_{\text{P/S}}$	Pick-up and set-down times of the elevators lifting table/shuttle carrier
t_1	Pick-up and set-down times in the first lane of the SBS/RS
t_2	Pick-up and set-down times in the second lane of the SBS/RS
t_x	Required travel time for the shuttle carrier to reach l
T_x	Required travel time for the shuttle carrier to reach L
t_y	Required travel time for the elevators lifting table to reach h
T_y	Required travel time for the elevators lifting table to reach H
$\lambda(\text{DCC})_{\text{SBS/RS}}$	SBS/RS system performance as a whole
Λ	Throughput performance
$\lambda(\text{SCC})_{\text{SCAR}}$	Throughput capacity of the single-command cycle of the shuttle carrier
$\lambda(\text{DCC})_{\text{SCAR}}$	Throughput capacity of the dual-command cycle of the shuttle carrier
$\lambda(\text{SCC})_{\text{LIFT1}}$	Throughput capacity of the single-command cycle of the elevator with one lifting table
$\lambda(\text{SCC})_{\text{LIFT2}}$	Throughput capacity of the single-command cycle of the elevator with two lifting tables
$\lambda(\text{DCC})_{\text{LIFT1}}$	Throughput capacity of the dual-command cycle of the elevator with one lifting table
$\lambda(\text{DCC})_{\text{LIFT2}}$	Throughput capacity of the dual-command cycle of the elevator with two lifting tables
t_p	Time necessary to reach the peak velocity
t	Travel time
vp_i	Velocity profile
$v(t)$	Velocity at time t
Q	Warehouse volume
w_{tote}	Width of the tote
w_{COM}	Width of the column

3.2 *Fundamentals of travel time*

Two types of velocity profiles can be distinguished depending on whether the obtained peak velocity $v(t_p)$ is less than $v_{\max}$ (type I) or equal to $v_{\max}$ (type II) (Figure 4). It can be verified that time $T < 2v_{\max}/a$ for type I and $T > 2v_{\max}/a$ for type II.

3.2.1 *Travelling for type I ($T < 2v_{\max}/a$)*

The velocity in dependence of time $v(t)$ is calculated by Equation (1):

$$v(t) = \begin{cases} at, & t \in (0, t_p) \\ -a(t-T), & t \in (t_p, T) \end{cases} \tag{1}$$

The distance in dependence of time $d(T)$ is calculated by Equation (2):

$$d(T) = \int_0^T v(t)\mathrm{d}t = \frac{a \cdot T^2}{4} \tag{2}$$

Because of the acceleration and deceleration are equal in magnitude, the time necessary to reach the peak velocity equals $t_p = T/2$.

3.2.2 *Travelling for type II ($\mathrm{T} > 2\mathrm{v}_{\max}/\mathrm{a}$)*

The velocity in dependence of time $v(t)$ is calculated by Equation (3):

$$v(t) = \begin{cases} at, & t \in (0, t_p) \\ v_{\max}, & t \in (t_p, T - t_p) \\ -a(t-T), & t \in (T - t_p, T) \end{cases} \tag{3}$$

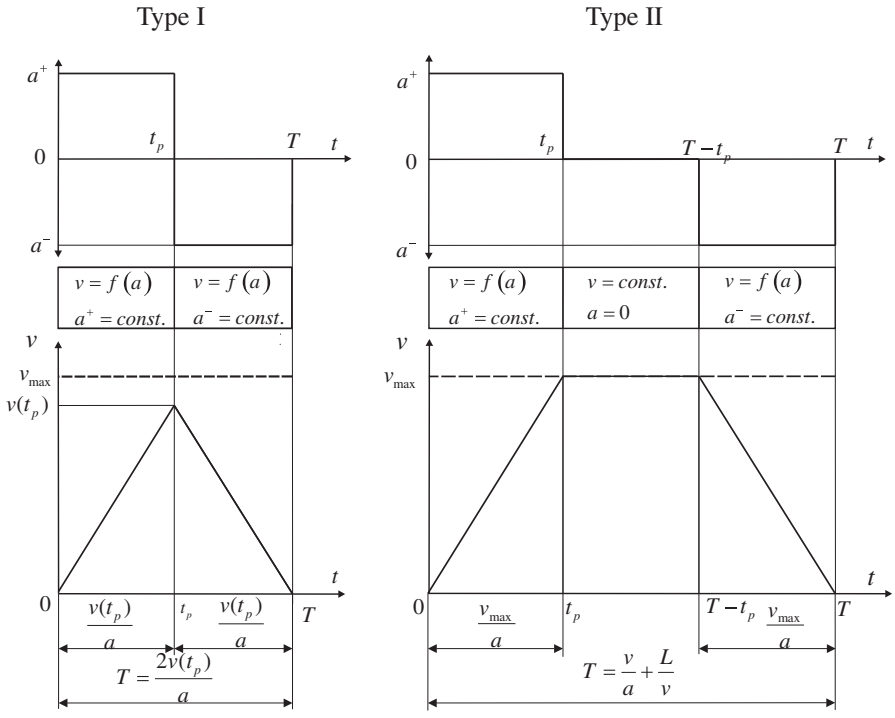

Figure 4. Velocity–time relationship (Lerher, Potrc et al. 2010).

The distance in dependence of time $d(T)$ is calculated by Equation (4):

$$d(T) = \int_0^T v(t)\mathrm{d}t = v_{\max} \cdot T - \frac{v_{\max}^2}{a} \tag{4}$$

3.3 *Travelling of the shuttle carrier in the SBS/RS*

Travel times of the shuttle carrier in the *i*th tier of the storage rack are variable times. They depend on the kinematics properties of the shuttle carrier, the length of the storage rack (*L)* and the storage policy. As regards to the condition of uniform distribution of storage locations in the storage rack, the cumulative distribution function ($F_x(t)$) is accomplished. The cumulative distribution function ($F_x(t)$) is distinguished according to the following condition.

- Travelling of the shuttle carrier from the $I/O_{tier(i)}$ location to randomly selected location in the *i*th tier of the storage rack

$$F_x(t) = \begin{cases} \dfrac{a_x t^2}{4L} & (0 \le t \le t_x) \\ \dfrac{v_x t}{L} - \dfrac{v_x^2}{a_x L} & (t_x \le t \le T_x) \end{cases} \tag{5}$$

- Travelling of the shuttle carrier from the storage location to the retrieval location in the *i*th tier of the storage rack

$$F_x(t) = \begin{cases} \dfrac{a_x}{2L} t^2 - \dfrac{a_x^2}{16L^2} t^4 & (0 \le t \le t_x) \\ -\dfrac{v_x^2}{L^2} t^2 + \left[\dfrac{2v_x^3}{a_x L^2} + \dfrac{2v_x}{L}\right] t - \dfrac{2v_x^2}{a_x L} - \dfrac{v_x^4}{a_x^2 L^2} & (t_x \le t \le T_x) \end{cases} \tag{6}$$

The cumulative distribution function ($F_x(t)$) depends on the relationships among the values of the following parameters: v_x, a_x, L. Therefore, $F(t)$ can be specified with the next expression:

$$F(t) = F_x(t) \quad \text{for } 0 \le t \le T_x \tag{7}$$

The expected travel time ($E(t)$) of the shuttle carrier is calculated by Equation (8):[1]

$$\mathrm{E}(t) = \int_0^{T_x} (1 - F(t))\mathrm{d}t \tag{8}$$

3.4 *Lifting of the elevators lifting table in the SBS/RS*

Travel times of the elevators lifting table of the SBS/RS are variable times. They depend from the kinematics properties of the elevators lifting table, the height of the storage rack (H) and the storage policy. As regards to the condition of uniform distribution of ith tiers of the SBS/RS, the cumulative distribution function ($F_y(t)$) is accomplished. The cumulative distribution function ($F_y(t)$) is distinguished according to the following condition:

- Lifting of the elevators lifting table from the I/O location to the ith tier of the SBS/RS

$$F_y(t) = \begin{cases} \dfrac{a_y t^2}{4H} & \left(0 \le t \le t_y\right) \\ \dfrac{v_y t}{H} - \dfrac{v_y^2}{a_y H} & \left(t_y \le t \le T_y\right) \end{cases} \tag{9}$$

- Lifting of the elevators lifting table from the ith tier to the jth tier of the SBS/RS

$$F_y(t) = \begin{cases} \dfrac{a_y}{2H} t^2 - \dfrac{a_y^2}{16H^2} t^4 & \left(0 \le t \le t_y\right) \\ -\dfrac{v_y^2}{H^2} t^2 + \left[\dfrac{2v_y^3}{a_y H^2} + \dfrac{2v_y}{H}\right] t - \dfrac{2v_y^2}{a_y H} - \dfrac{v_y^4}{a_y^2 H^2} & \left(t_y \le t \le T_y\right) \end{cases} \tag{10}$$

The cumulative distribution function ($F_y(t)$) depends on the relationships among the values of the following parameters: v_y, a_y, H. Therefore, $F(t)$ can be specified with the next expression:

$$F(t) = F_y(t) \quad \text{for } 0 \le t \le T_y \tag{11}$$

The expected travel time ($E(t)$) of the elevators lifting table is calculated by Equation (12):[2]

$$\mathrm{E}(t) = \int_0^{T_y} (1 - F(t))\mathrm{d}t \tag{12}$$

4. Travel time model for double-deep SBS/RS

In case of double-deep SBS/RS, the average travel time for the single- and the dual-command cycle is enlarged for the rearrangement of the blocking totes to the nearest free storage location in the storage rack. When developing the proposed analytical travel time model for double- deep SBS/RS, the assumptions, presented in FEM 9.851 guideline, have been considered. The FEM 9.851 (1978) guideline introduces the condition that the rearrangement of the blocking totes can occur during the storage and retrieval assignment. It was assumed that during the storage assignment in the first or in the second storage lane, the totes will be always stored first in the second lane. When all storage locations in the second lane are occupied, then the storage in the first lane begins. According to the latter, the possibility of the rearrangement of the blocking totes is eliminated. On the contrary, in the case of retrieval process, the access to the second lane might be blocked by the blocking totes in the first lane (a special case of retrieval). The problem can be solved by rearranging the blocking totes to the nearest free storage location in the storage rack. Rearrangement of totes is performed by the next sequence: pick up the blocking tote (single-depth); repositioning of the shuttle carrier to the nearest free storage location; set down the formerly blocking tote (single- or double-depth); repositioning of the shuttle carrier to the

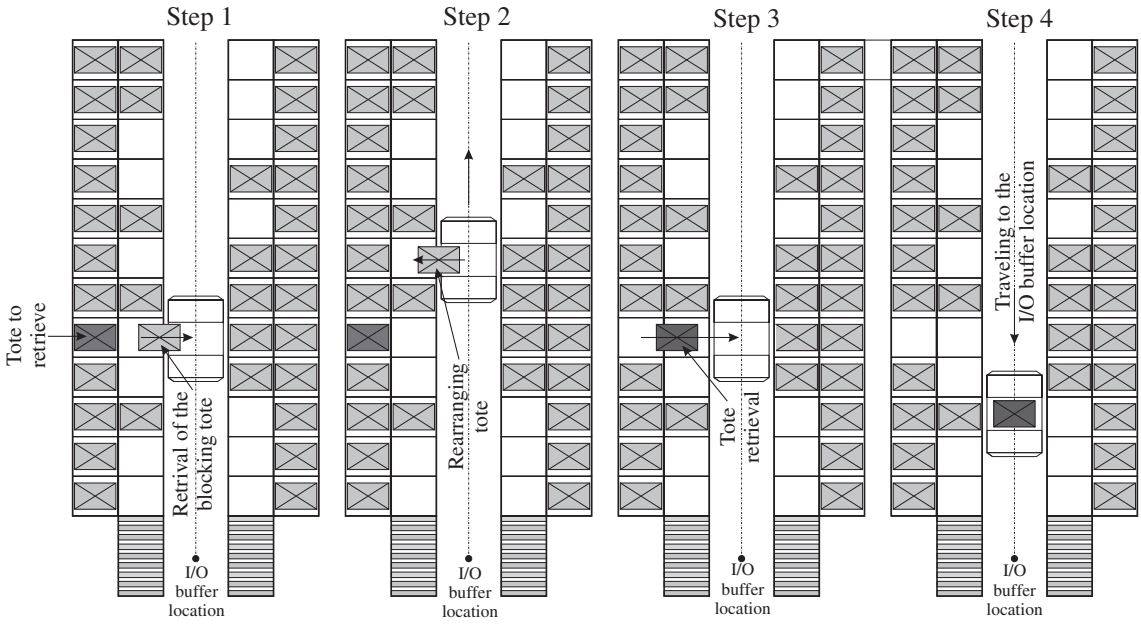

Figure 5. The procedure of rearranging a tote in the SBS/RS during the retrieval assignment.

earlier retrieval location; pick up the tote to retrieve (double-depth) Ritonja (2003), Oser and Ritonja (2004), Lerher, Sraml et al. (2010) (Figure 5).

Rearranging blocking totes to the nearest free storage location is influenced by:

- fill-grade factor α, which has an effect on the rearrangement distances and number of rearrangements.
- storage strategy.

4.1 *The definition of the rearrangement distance*

The average rearrangement distance and consequently the average travel time to the nearest free storage location in the storage rack, using the randomised storage assignment rule, is influenced by the fill-grade factor α. In the proposed analytical travel time model for the calculation of the average rearrangement distance, the FEM 9.851 guideline and the results of simulation modelling analysis have been used (Ritonja 2003).

The expected value of the rearrangement distances in the ith tier of the SBS/RS is calculated by Equation (13):

$$E_x = \frac{1}{3} \cdot \frac{L}{n_x} \sqrt{\frac{1}{(1-\alpha)}} \tag{13}$$

The fill-grade factor is calculated from the next relationship:

$$\alpha = \frac{n_{\text{stored}}}{n_{\text{total}}} \tag{14}$$

4.2 *The influence of the fill-grade factor α on the rearrangement assignment*

4.2.1 *The introduction of the storage strategy with the fill-grade factor α [0, 0.5]*

In continuation, the following assumptions were considered (Ritonja 2003):

- totes will always be first stored in the second lane of the SBS/RS,
- when all storage locations in the second lane of the SBS/RS are full ($\alpha > 0.5$), the storage assignment in the first storage lane of the SBS/RS begins,
- possibility of the rearrangement of the blocking tote is eliminated during the storage and the retrieval processes in the SBS/RS.

• Second lane of the SBS/RS

The probability $P_{\text{Occ.}}$ that the storage location in the second lane of the SBS/RS is occupied (Ritonja 2003), is calculated by Equation (15):

$$P_{\text{Occ.}} = 2\alpha \tag{15}$$

The probability P_{Free} that the storage location in the second lane of the SBS/RS is empty (Ritonja 2003), is calculated by Equation (16):

$$P_{\text{Free}} = 1 - 2\alpha \tag{16}$$

- First lane of the SBS/RS

The probability $P_{\text{Occ.}}$ that the storage location in the first lane of the SBS/RS is occupied (Ritonja 2003), is calculated by Equation (17):

$$P_{\text{Occ.}} = 0 \tag{17}$$

The probability P_{Free} that the storage location in the first lane of the SBS/RS is empty (Ritonja 2003), is calculated by Equation (18): (Figure 6)

$$P_{\text{Free}} = 1 \tag{18}$$

According to the value of the fill-grade factor α, which can be in the range from [0 to 0.5] two different cases of the storage and retrieval assignment can occur during the working cycle (Ritonja 2003) (Figure 7).

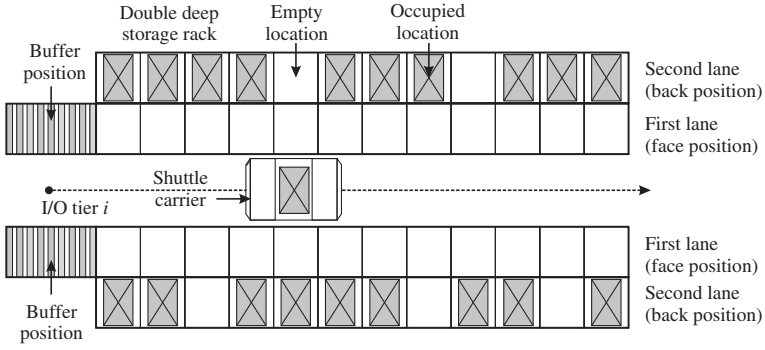

Figure 6. The layout of the double-deep SBS/RS with the fill-grade factor α [0, 0.5].

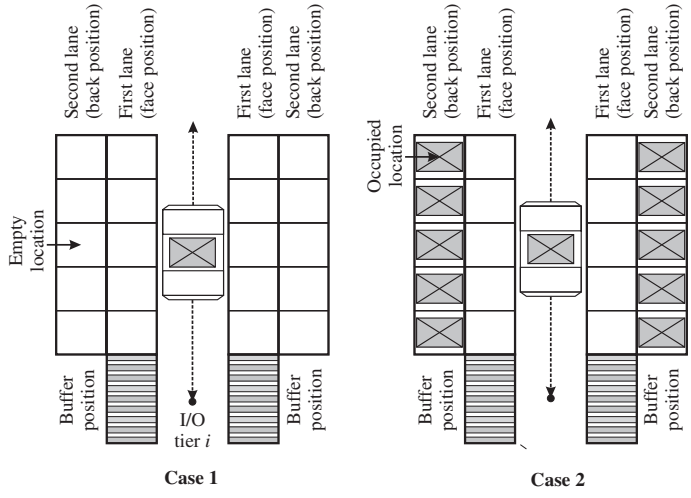

Figure 7. Two different cases of the storage and retrieval assignments in the double-deep SBS/RS in case of the fill grade factor α [0, 0.5].

Case 1 *(the first and the second lane of the SBS/RS are both free)*
The probability P_1 that the storage locations in the first and in the second lane of the SBS/RS are empty (Ritonja 2003), is calculated by Equation (19):

$$P_1 = P_{\text{Free}} \cdot P_{\text{Free}} = 1 - 2\alpha \tag{19}$$

Case 2 *(the first lane of the SBS/RS is empty, while the second lane of the SBS/RS is occupied)*
The probability P_2 that the storage locations in the first lane of the SBS/RS are empty and occupied in the second lane of the SBS/RS (Ritonja 2003), is calculated by Equation (20):

$$P_2 = P_{\text{Free}} \cdot P_{\text{Occ.}} = 2\alpha \tag{20}$$

4.2.2 *The introduction of the storage strategy with the fill-grade factor* α *[0.5, 1]*

In continuation, the following assumptions were considered (Ritonja 2003):

- because all storage locations in the second lane of the SBS/RS are full ($\alpha > 0.5$), the storage in the first lane of the SBS/RS begins,
- possibility of the rearrangement of the blocking tote is eliminated during the storage assignment,
- because of the second lane of the SBS/RS might be blocked by the blocking totes in the first lane of the SBS/RS, the rearrangement of the blocking totes to the nearest free storage location during the retrieval process is introduced.

• Second lane of the SBS/RS

The probability $P_{\text{Occ.}}$ that the storage location in the second lane of the SBS/RS is occupied (Ritonja 2003), is calculated by Equation (21):

$$P_{\text{Occ.}} = 1 \tag{21}$$

The probability P_{Free} that the storage location in the second lane of the SBS/RS is empty (Ritonja 2003), is calculated by Equation (22):

$$P_{\text{Free}} = 0 \tag{22}$$

• First lane of the SBS/RS

The probability $P_{\text{Occ.}}$ that the storage location in the first lane of the SBS/RS is occupied (Ritonja 2003), is calculated by Equation (23):

$$P_{\text{Occ.}} = 2\alpha - 1 \tag{23}$$

The probability P_{Free} that the storage location in the first lane of the SBS/RS is empty (Ritonja 2003), is calculated by Equation (24): (Figure 8)

$$P_{\text{Free}} = 2 - 2\alpha \tag{24}$$

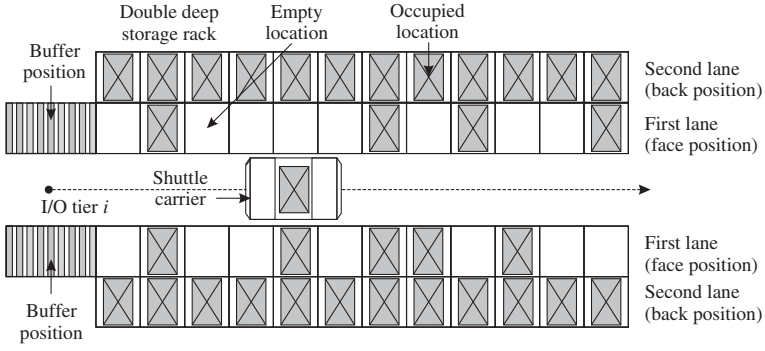

Figure 8. The layout of the double-deep SBS/RS with the fill-grade factor α [0.5, 1.0].

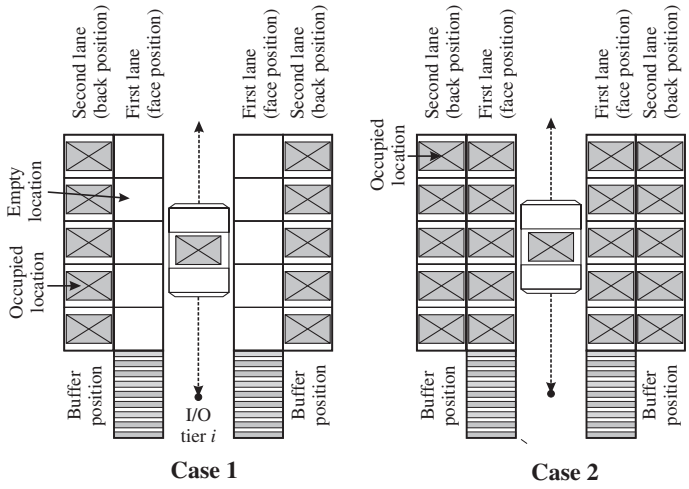

Figure 9. Two different cases of the storage and retrieval assignments in the double-deep SBS/RS in case of the fill grade factor α [0.5, 1.0].

According to the value of the fill-grade factor α, which can be in the range from 0.5 to 1.0, two different cases of the storage and retrieval assignment can occur during the working cycle (Ritonja 2003) (Figure 9).

Case 2 *(the first lane of the SBS/RS is empty, while the second lane of the SBS/RS is occupied)*
The probability P_2 that the storage locations in the first lane of the SBS/RS are empty and occupied in the second lane of the SBS/RS (Ritonja 2003), is calculated by Equation (25):

$$P_2 = P_{\text{Free}} \cdot P_{\text{Occ.}} = 2 - 2\alpha \tag{25}$$

Case 3 *(the first and the second lane of the SBS/RS are both occupied)*
The probability P_3 that the storage locations in the first and in the second lane of the SBS/RS are occupied (Ritonja 2003), is calculated by Equation (26):

$$P_3 = P_{\text{Occ.}} \cdot \ P_{\text{Occ.}} = 2\alpha - 1 \tag{26}$$

4.3 *Cycle time of the shuttle carrier in double-deep AS/RS when α [0, 0.5]*

4.3.1 *The probability of rearrangements during the storage and retrieval processes*

According to the assumption in chapter 3.1, the probability of rearrangement during the storage and the retrieval assignments, is equal to the following expression (Ritonja 2003):
Storage assignment

$$P_{R(\text{storage})} = 0 \tag{27}$$

Retrieval assignment

$$P_{R(\text{retrieval})} = 0 \tag{28}$$

Because of the assumption that the probability of the rearrangement during the storage and the retrieval assignments equals to zero, the probability P_R of the rearrangement of totes during the single and the dual-command cycles equals to 0.

4.3.2 *Single-command cycle (single storage or single retrieval)*

Single-command cycle involves either storage or retrieval assignment operation. Single-command cycle in case of α [0, 0.5] consists of time for picking up the tote at the $I/O_{\text{tier}(i)}$ location (start position), travelling to the destination position and setting down the TUL in the second storage lane of the storage rack, returning empty to the start position and setting down the tote at the $I/O_{\text{tier}(i)}$ location (Figure 10).

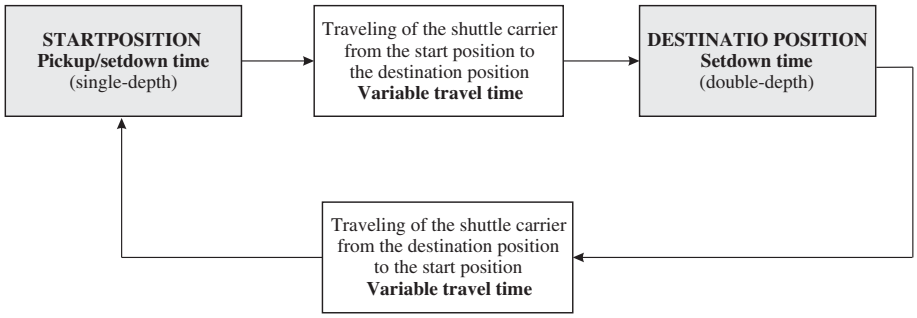

Figure 10. Single-command cycle of the shuttle carrier with the fill-grade factor α [0, 0.5].

The expected single-command cycle time ($E(\mathrm{SCC})_{\mathrm{SCAR}}$) is calculated by Equation (29):

$$E(\mathrm{SCC})_{\mathrm{SCAR}} = 2 \cdot t_{\mathrm{P/S}} + 2 \cdot E(\mathrm{ES})_{\mathrm{SCAR}} + t_2 \tag{29}$$

where, $t_{\mathrm{P/S}}$, pick-up and set-down times at the $\mathrm{I/O}_{\mathrm{tier}(i)}$ location; $E(\mathrm{ES})_{\mathrm{SCAR}}$expected travel time from the start position $\mathrm{I/O}_{\mathrm{tier}(i)}$ to the destination position s_i; t_2, pick-up and set-down times in the second lane of the SBS/RS.

Throughput capacity $\lambda(\mathrm{SCC})_{\mathrm{SCAR}}$ of the single-command cycle is calculated by Equation (30):

$$\lambda(\mathrm{SCC})_{\mathrm{SCAR}} = \frac{3600}{E(\mathrm{SCC})_{\mathrm{SCAR}}} \tag{30}$$

4.3.3 *Dual-command cycle (single storage and single retrieval in the cycle)*

Dual-command cycle involves both storage and retrieval operations simultaneously. Dual-command cycle time consists of the time for picking up the tote at the $\mathrm{I/O}_{\mathrm{tier}(i)}$ location, travelling to the destination position and setting down the tote in the second lane of the SBS/RS, travelling empty to the retrieval position, retrieving the tote from the second lane of the SBS/RS and returning to the start position and setting down the tote at the $\mathrm{I/O}_{\mathrm{tier}(i)}$ location (Figure 11).

The expected dual-command cycle time ($E(\mathrm{DCC})_{\mathrm{SCAR}}$) is calculated by Equation (31):

$$E(\mathrm{DCC})_{\mathrm{SCAR}} = 2 \cdot t_{\mathrm{P/S}} + 2 \cdot E(\mathrm{ES})_{\mathrm{SCAR}} + E(\mathrm{TB})_{\mathrm{SCAR}} + 2t_2 \tag{31}$$

where, $t_{\mathrm{P/S}}$, pick-up and set-down times at the $\mathrm{I/O}_{\mathrm{tier}(i)}$ location; $E(\mathrm{ES})_{\mathrm{SCAR}}$, expected travel time from the start position $\mathrm{I/O}_{\mathrm{tier}(i)}$ to the destination position s_i; $E(\mathrm{TB})_{\mathrm{SCAR}}$, expected travel time from the storage position s_i to the retrieval position r_i; t_2, pick-up and set-down times in the second storage lane of the SBS/RS.

Throughput capacity $\lambda(\mathrm{DCC})_{\mathrm{SCAR}}$ of the dual-command cycle is calculated by Equation (32):

$$\lambda(\mathrm{DCC})_{\mathrm{SCAR}} = \frac{3600}{E(\mathrm{DCC})_{\mathrm{SCAR}}} \cdot 2 \tag{32}$$

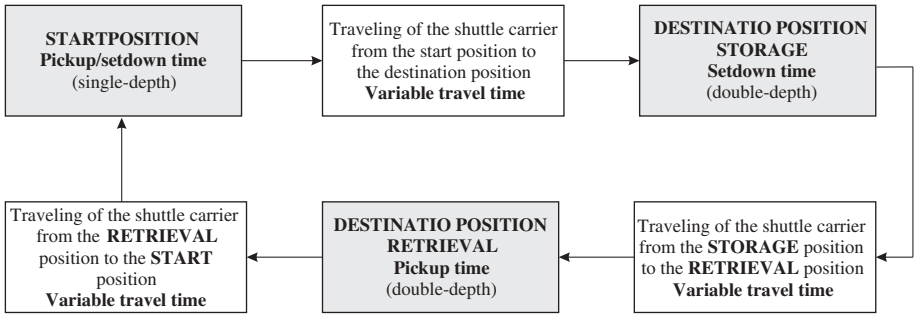

Figure 11. Dual-command cycle of the shuttle carrier with the fill-grade factor α [0, 0.5].

4.4 *Cycle time of the shuttle carrier in double deep AS/RS when α [0.5, 1.0]*

4.4.1 *Single-command cycle*

4.4.1.1 *Single storage assignment.* Single storage assignment consists of the time for picking up the tote at the $I/O_{tier(i)}$ location, travelling to the destination position and setting down the tote in the first lane of the SBS/RS, returning empty to the start position and setting down the tote at the $I/O_{tier(i)}$ location (Figure 12).

The expected single-command cycle time $E(SCC)_{SCAR}$, in case of storage assignment, is calculated by Equation (33):

$$E(SCC)_{SCAR} = 2 \cdot t_{P/S} + 2 \cdot E(ES)_{SCAR} + t_1 \tag{33}$$

$t_{P/S}$, pick up and set down times at the $I/O_{tier(i)}$ location; $E(ES)_{SCAR}$, expected travel time from the start position $I/O_{tier(i)}$ to the destination position s_i; t_1, pick-up and set-down times in the first lane of the SBS/RS.

Throughput capacity ($\lambda(SCC)_{SCAR}$) of the single-command cycle is calculated by Equation (34):

$$\lambda(SCC)_{SCAR} = \frac{3600}{E(SCC)_{SCAR}} \tag{34}$$

4.4.1.2 *Single retrieval assignment.* For the single retrieval assignment, the single-command cycle consists of the time of shuttle carrier travelling empty to the destination position in the double deep SBS/RS, retrieving the tote from the first or the second lane of the SBS/RS, returning to the start position and setting down the tote at the $I/O_{tier(i)}$ location. Because totes are stored in the first and in the second lanes of the SBS/RS, the access to the second lane might be blocked by the blocking tote. When a blockade occurs, the shuttle carrier has to pick up the blocking tote from the first lane and of the SBS/RS, rearrange it to the nearest free position, which can be either in the first or in the second lane of the SBS/RS. Therefore, instead of the regular retrieval time, the additional time for the rearrangement is attached (Figure 13).

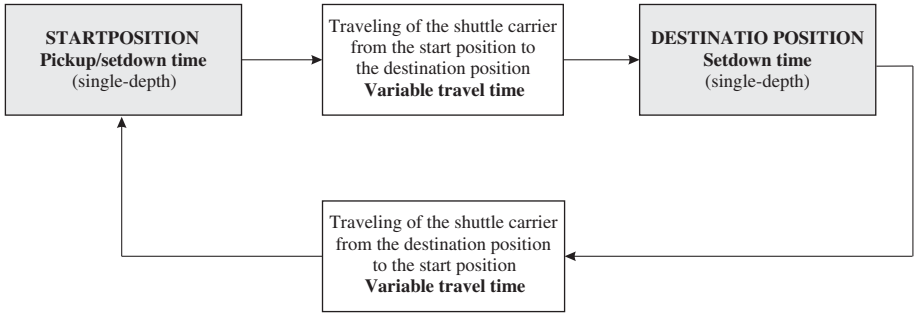

Figure 12. Single storage assignment of the shuttle carrier with the fill-grade factor α [0.5, 1.0].

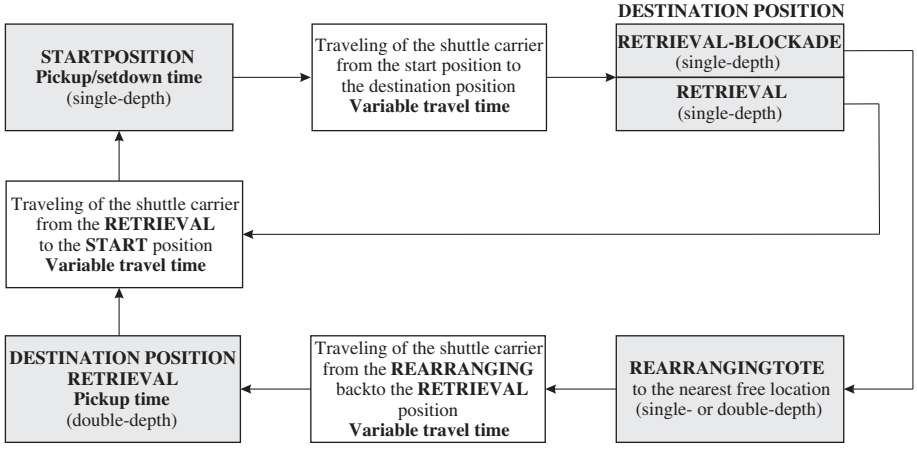

Figure 13. Single retrieval assignment of the shuttle carrier with the fill-grade factor α [0.5, 1.0]

The expected single-command cycle time $E(\mathrm{SCC})_{\mathrm{SCAR}}$, in case of retrieval assignment, is calculated by Equation (35):

$$\begin{aligned} E(\mathrm{SCC})_{\mathrm{SCAR}} &= E(\mathrm{SCC})_{\mathrm{SCAR}} + \frac{\alpha}{2} E(\mathrm{R}) \\ E(\mathrm{SCC})_{\mathrm{SCAR}} &= 2 \cdot t_{\mathrm{P/S}} + 2 \cdot E(\mathrm{ES})_{\mathrm{SCAR}} + (P_1 \cdot t_1 + P_2 \cdot t_2) + \frac{\alpha}{2}[2 \cdot E(t_R) + t_1 + (P_1 \cdot t_1 + P_2 \cdot t_2)] \end{aligned} \tag{35}$$

where, t_{PD}, pick-up and set-down times at the $\mathrm{I/O}_{\mathrm{tier}(i)}$ location; $E(\mathrm{ES})_{\mathrm{SCAR}}$, expected travel time from the start position $\mathrm{I/O}_{\mathrm{tier}(i)}$ to the destination position r_i; P_1, probability of retrieval in the first lane of the SBS/RS; t_1, pick-up and set-down times in the first lane of the SBS/RS; P_2, probability of retrieval in the second storage lane of the SBS/RS; t_2, pick-up and set-down times in the second storage lane of the SBS/RS; $E(R)$, expected rearrangement cycle time; $E(t_R)$, expected travel time from the retrieval position to the rearrangement position.

The probability P_1 (Ritonja 2003), which stands for the condition that the tote will be pick up and set down from the first lane of the SBS/RS, is calculated by Equation (36):

$$P_1 = \frac{P_3}{P_2 + 2\mathrm{P}_3} = \frac{2\alpha - 1}{2 - 2\alpha + 2(2\alpha - 1)} = \frac{2\alpha - 1}{2\alpha} \tag{36}$$

The probability P_2 (Ritonja 2003), which stands for the condition that the tote will be pick up and set down from the second lane of the SBS/RS, is calculated by Equation (37):

$$P_2 = \frac{P_2}{P_2 + 2\mathrm{P}_3} + \frac{P_3}{P_2 + 2\mathrm{P}_3} = \frac{2 - 2\alpha}{2 - 2\alpha + 2(2\alpha - 1)} + \frac{2\alpha - 1}{2 - 2\alpha + 2(2\alpha - 1)} = \frac{1}{2\alpha} \tag{37}$$

The expected single-command cycle time $E(\mathrm{SCC})_{\mathrm{SCAR}}$ is calculated by Equation (38):

$$E(\mathrm{SCC})_{\mathrm{SCAR}} = 2 \cdot t_{\mathrm{P/S}} + 2 \cdot E(\mathrm{ES})_{\mathrm{SCAR}} + \left(\left(\frac{2\alpha - 1}{2\alpha}\right) \cdot t_1 + \left(\frac{1}{2\alpha}\right) \cdot t_2\right) + \frac{\alpha}{2}\left[2 \cdot E(t_R) + \left(\left(\frac{4\alpha - 1}{2\alpha}\right) \cdot t_1 + \left(\frac{1}{2\alpha}\right) \cdot t_2\right)\right] \tag{38}$$

Throughput capacity $\lambda(\mathrm{SCC})_{\mathrm{SCAR}}$ of the single-command cycle is calculated by Equation (39):

$$\lambda(\mathrm{SCC})_{\mathrm{SCAR}} = \frac{3600}{E(\mathrm{SCC})_{\mathrm{SCAR}}} \tag{39}$$

4.4.2 *Dual-command cycle*

Dual-command cycle involves both storage and retrieval operations simultaneously. Dual-command cycle time consists of the time to pick up the tote at the $\mathrm{I/O}_{\mathrm{tier}(i)}$ location, travel to the destination position and set down the tote in the first lane of the SBS/RS, travel empty to the retrieval position, retrieve the tote from the first or the second lane of the SBS/RS, return to the start position and set down the tote at the $\mathrm{I/O}_{\mathrm{tier}(i)}$ location. During the retrieval process rearrangement of the blocking tote can occur (Figure 14).

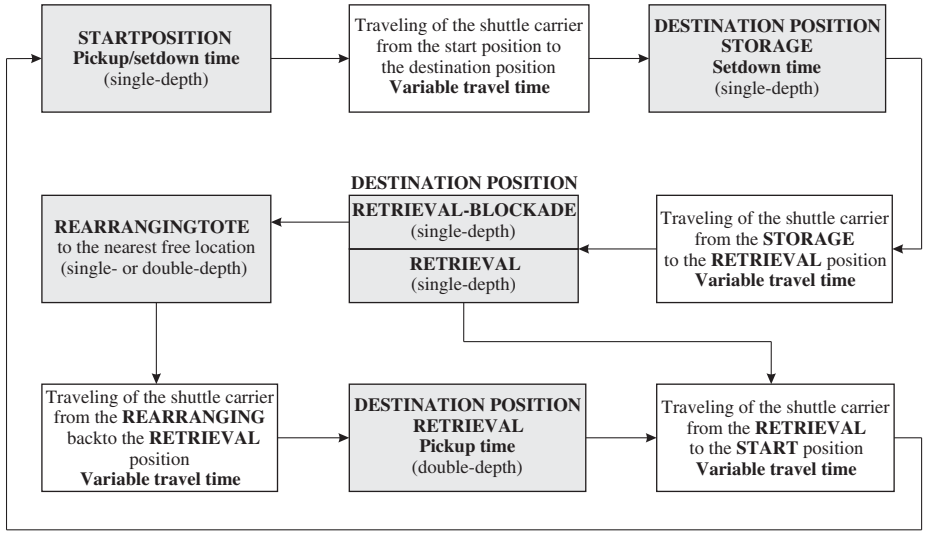

Figure 14. Dual-command cycle of the shuttle carrier with the fill-grade factor α [0.5, 1.0].

The expected dual-command cycle time $E(\mathrm{DCC})_{\mathrm{SCAR}}$ with rearranging totes is calculated by Equation (40):

$$E(\mathrm{DCC})_{\mathrm{SCAR}} = 2 \cdot t_{\mathrm{P/S}} + 2 \cdot E(\mathrm{ES})_{\mathrm{SCAR}} + t_1 + E(\mathrm{TB})_{\mathrm{SCAR}} + (P_1 \cdot t_1 + P_2 \cdot t_2) + \frac{\alpha}{2}[2 \cdot E(t_R) + t_1 + (P_1 \cdot t_1 + P_2 \cdot t_2)] \tag{40}$$

where, $t_{\mathrm{P/S}}$, pick-up and set-down times at the $\mathrm{I/O}_{\mathrm{tier}(i)}$ location; $E(\mathrm{ES})_{\mathrm{SCAR}}$, expected travel time from the start position $\mathrm{I/O}_{\mathrm{tier}(i)}$ to the destination position; $E(\mathrm{TB})_{\mathrm{SCAR}}$, expected travel time from the storage position s_i to the retrieval position r_i; P_1, probability of retrieval in the first lane of the SBS/RS; t_1, pick-up and set-down times in the first lane of the SBS/RS; P_2, probability of retrieval in the second storage lane of the SBS/RS; t_2, pick-up and set-down times in the second storage lane of the SBS/RS; $E(t_R)$, expected travel time from the retrieval position to the rearrangement position.

The expected dual-command cycle time $E(\mathrm{DCC})_{\mathrm{SCAR}}$ is calculated by Equation (41):

$$E(\mathrm{DCC})_{\mathrm{SCAR}} = 2 \cdot t_{\mathrm{P/S}} + 2 \cdot E(\mathrm{ES})_{\mathrm{SCAR}} + E(\mathrm{TB})_{\mathrm{SCAR}} + \left(\left(\frac{4\alpha - 1}{2\alpha}\right) \cdot t_1 + \left(\frac{1}{2\alpha}\right) \cdot t_2\right) + \frac{\alpha}{2}\left[2 \cdot E(t_R) + \left(\left(\frac{4\alpha - 1}{2\alpha}\right) \cdot t_1 + \left(\frac{1}{2\alpha}\right) \cdot t_2\right)\right] \tag{41}$$

Throughput capacity $\lambda(\mathrm{DCC})_{\mathrm{SCAR}}$ of the dual-command cycle is calculated by Equation (42):

$$\lambda(\mathrm{DCC})_{\mathrm{SCAR}} = \frac{3600}{E(\mathrm{DCC})_{\mathrm{SCAR}}} \cdot 2 \tag{42}$$

4.5 *Cycle time of the elevators lifting table in double deep AS/RS*

4.5.1 *Single-command cycle*

Single-command cycle involves either storage or retrieval assignment operation. Single-command cycle consists of the time for picking up the tote at the I/O location (start position), moving of the elevators lifting table to the *i*th tier of the SBS/RS and setting down the tote to the buffer location. This assignment can be done vice versa as well (Figure 15).

The expected single-command cycle time $E(\mathrm{SCC})_{\mathrm{LIFT}}$ is calculated by Equation (43):

$$E(\mathrm{SCC})_{\mathrm{LIFT}} = 2 \cdot t_{\mathrm{P/S}} + 2 \cdot E(\mathrm{ES})_{\mathrm{LIFT}} \tag{43}$$

where, $t_{\mathrm{P/S}}$, pick up and set down times at the I/O location; $E(\mathrm{ES})_{\mathrm{LIFT}}$, expected travel time from the I/O location to the *i*th tier of the SBS/RS.

Throughput capacity $\lambda(\mathrm{SCC})_{\mathrm{LIFT1}}$ of the single-command cycle with the elevator with one lifting table only is calculated by Equation (44):

$$\lambda(\mathrm{SCC})_{\mathrm{LIFT1}} = \frac{3600}{E(\mathrm{SCC})_{\mathrm{LIFT}}} \tag{44}$$

Throughput capacity $\lambda(\mathrm{SCC})_{\mathrm{LIFT2}}$ of the single-command cycle with the elevator with two lifting tables is calculated by Equation (45):

$$\lambda(\mathrm{SCC})_{\mathrm{LIFT2}} = 2 \cdot \lambda(\mathrm{SCC})_{\mathrm{LIFT1}} \tag{45}$$

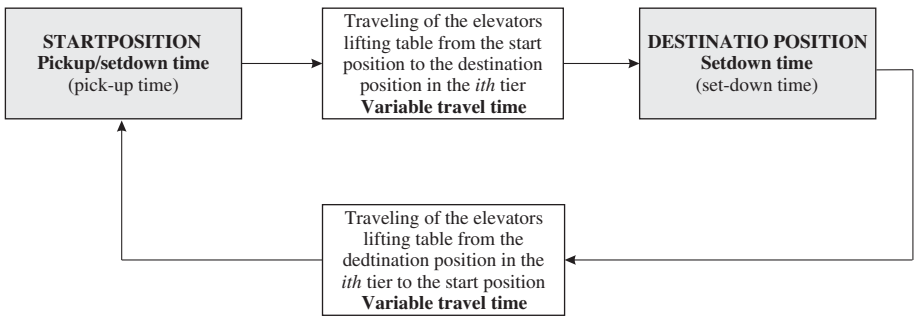

Figure 15. Single-command cycle of the elevators lifting table.

4.5.2 *Dual-command cycle*

Dual-command cycle involves both storage and retrieval assignments simultaneously. Dual-command cycle time consists of the time for picking up the tote at the I/O location, moving of the elevators lifting table to the *i*th tier of the SBS/RS and setting down the tote to the buffer location, moving empty to the retrieval position in the *j*th tier of the SBS/RS and retrieving the tote from the buffer location and returning to the start position and setting down the tote at the I/O location (Figure 16).

The expected dual-command cycle time $E(\mathrm{DCC})_{\mathrm{LIFT}}$ is calculated by Equation (46):

$$E(\mathrm{DCC})_{\mathrm{LIFT}} = 2 \cdot t_{\mathrm{P/S}} + 2 \cdot E(\mathrm{ES})_{\mathrm{LIFT}} + E(\mathrm{TB})_{\mathrm{LIFT}} \tag{46}$$

where, $t_{\mathrm{P/S}}$, pick-up and set-down times at the I/O location; $E(\mathrm{ES})_{\mathrm{LIFT}}$, expected travel time from the I/O location to the *i*th tier of the SBS/RS; $E(\mathrm{TB})_{\mathrm{LIFT}}$, expected travel time from the storage position in the *i*th tier of the SBS/RS, to the retrieval position in the *j*th tier of the SBS/RS.

Throughput capacity $\lambda(\mathrm{DCC})_{\mathrm{LIFT1}}$ of the dual-command cycle with the elevator with one lifting table only is calculated by Equation (47):

$$\lambda(\mathrm{DCC})_{\mathrm{LIFT1}} = \frac{3600}{E(\mathrm{DCC})_{\mathrm{LIFT}}} \cdot 2 \tag{47}$$

Throughput capacity $\lambda(\mathrm{DCC})_{\mathrm{LIFT2}}$ of the dual-command cycle with the elevator with two lifting tables is calculated by Equation (48):

$$\lambda(\mathrm{DCC})_{\mathrm{LIFT2}} = 2 \cdot \lambda(\mathrm{DCC})_{\mathrm{LIFT1}} \tag{48}$$

5. Double-deep SBS/RS under study

5.1 *Main input data for the analysis*

In this section, main input data for the analysis are provided and discussed. Stock keeping unit represents a tote with the following dimensions: length $l_{\mathrm{tote}} = 0.6$ m, width $w_{\mathrm{tote}} = 0.4$ m and height $h_{\mathrm{tote}} = 0.24$ m. With regard to the tote, the storage location has the following dimensions: length (depth) of the column $l_{\mathrm{COM}} = 0.6$ m, width of the column $w_{\mathrm{COM}} = 0.5$ m and height of the column (tier) $h_{\mathrm{COM}} = 0.5$ m. Dimensions of the SBS/RS storage rack (L and H) depends on the number of columns C in the horizontal direction and number of tiers M in the vertical direction, respectively.

Since the throughput capacity λ greatly depends on the velocity characteristics of the elevators lifting table and the shuttle carrier, three different velocity profile vp_i ($i = 1, \ldots, 3$) scenarios are analysed (Table 1).

Other data that are used in the analyses are presented in Table 2.

5.2 *Analysis and evaluation of results*

In this section, travel time analysis and the throughput performance for the selected double- deep SBS/RS are presented. Analysis is performed by considering selected SBS/RS (Table 3) and velocity profiles vp_i (Table 1) of the shuttle carrier and the elevators lifting table.

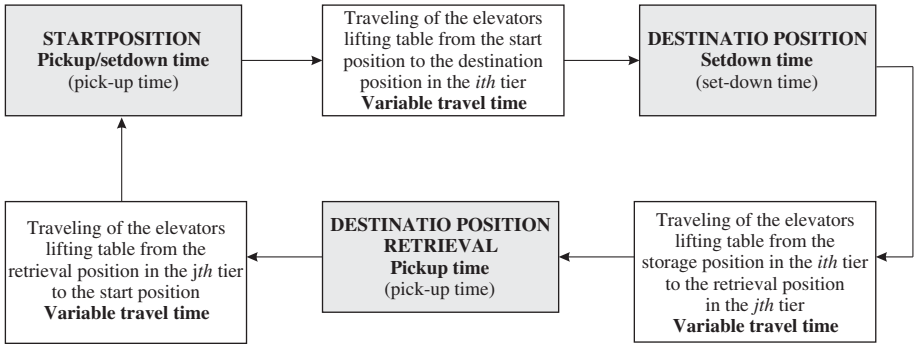

Figure 16. Dual-command cycle of the elevators lifting table.

Table 1. Velocity scenarios of the shuttle carrier and the elevators lifting table.

	Shuttle carrier travelling in the horizontal direction			Lifting table movement in the vertical direction		
Velocity profile	v_x (m/s)	a_x^+ (m/s^2)	a_x^- (m/s^2)	v_y (m/s)	a_y^+ (m/s^2)	a_y^- (m/s^2)
vp_1	1.5	1.5	1.5	1.5	1.5	1.5
vp_2	3.0	2.0	2.0	2.0	1.5	1.5
vp_3	4.0	3.0	3.0	2.5	2.0	2.0

Note: Velocity scenarios vp_1, vp_2 and vp_3 were selected according to the references of material handling equipment producers and practical experiences of the authors.

Table 2. Other data used in the analysis.

Variable	Unit of measure	Data
$t_{P/S}$ (lift)	s	1.5
$t_{P/S}$ (shuttle carrier)	s	3.4
t_1 (shuttle carrier)	s	3.4
t_2 (shuttle carrier)	s	5.8

Table 3. Double-deep SBS/RS configuration.

SBS/RS configuration	Number of tiers (M)	Number of aisles (A)	Number of columns (C)	Length of the SR (L)	Height of the SR (H)	Warehouse volume (Q)
1	12	1	60	30	6	2880

Note: Double-deep SBS/RS configuration is selected according to the references of material handling equipment producers and practical experiences of the authors.

5.2.1 *Travel time and throughput performance of the shuttle carrier*

Expected dual-command cycle times and throughput capacities of the shuttle carrier for the selected double-deep SBS/RS, are given on the basis of the performed analysis. Analysis has been conducted for the chosen SBS/RS presented in Table 3, under the condition of the possible rearrangement of the blocking tote during the retrieval assignment process. In order to receive the best representative results, the double-deep SBS/RS corresponds to a fill-grade factor $\alpha = 0.55$, 0.60, 0.65, 0.70, 0.75, 0.80, 0.85, 0.95 and 0.99 (Table 4).

Expected dual-command cycle time $E(\mathrm{DCC})_{\mathrm{SCAR}}$ and consequently throughput performance $\lambda(\mathrm{DCC})_{\mathrm{SCAR}}$ of the shuttle carrier depend on the selected SBS/RS and the velocity profile vp_i of the shuttle carrier (v_x and a_x).

According to the distribution of the $E(\mathrm{DCC})_{\mathrm{SCAR}}$, velocity vp_i has a significant impact on the expected dual-command cycle time of the shuttle carrier. In $E(\mathrm{DCC})_{\mathrm{SCAR}}$ distribution, significant decreasing tendency of $E(\mathrm{DCC})_{\mathrm{SCAR}}$ is observed for the velocity profile vp_3 according to the velocity profile vp_1 and vp_2. This relationship shows the influence of horizontal velocity v_x and acceleration a_x in accordance to the length L of the SBS/RS. Since the length L of the SBS/RS is usually relatively long, the shuttle carrier in most of cases reaches the maximum velocity, which has a consequence on the travel (cycle) time. Generally, the best results are achieved by shuttle carriers having fast drivers in the horizontal travelling direction.

Because the throughput capacity $\lambda(\mathrm{DCC})_{\mathrm{SCAR}}$ of the shuttle carrier is inversly dependent on the expected dual-command cycle time $E(\mathrm{DCC})_{\mathrm{SCAR}}$, the highest throughput capacity $\lambda(\mathrm{DCC})_{\mathrm{SCAR}}$ belongs to the SBS/RS with the shuttle carrier having the highest horizontal velocity v_x. On the contrary, the lowest throughput capacity $\lambda(\mathrm{DCC})_{\mathrm{SCAR}}$ belongs to the SBS/RS with the shuttle carrier having the low horizontal velocity v_x.

According to the increased fill-grade factor α, an increasing trend of the expected dual-command cycle time $E(\mathrm{DCC})_{\mathrm{SCAR}}$ can be noticed. This relationship can be explained by the increasing length of the rearrangement distances, which causes the enlargement of the rearrangement time and consequently the travel (cycle) time. Because the throughput performance $\lambda(\mathrm{DCC})_{\mathrm{SCAR}}$ of the SBS/RS is inversely dependant on the expected dual-command cycle time $E(\mathrm{DCC})_{\mathrm{SCAR}}$, the decreasing trend of throughput capacities $\lambda(\mathrm{DCC})_{\mathrm{SCAR}}$ with regard to the increased fill-grade factor α, can be noticed.

Table 4. Travel time and throughput performance of the shuttle carrier.

Velocity profile vp_i	Fill-grade factor α	Cycle time of the shuttle carrier $E(\mathrm{DCC})_{\mathrm{SCAR}}$	Throughput performance of the shuttle carrier $\lambda(\mathrm{DCC})_{\mathrm{SCAR}}$
vp_1	0.55	48.33	149
	0.60	48.37	149
	0.65	48.45	149
	0.70	48.55	148
	0.75	48.69	148
	0.80	48.85	147
	0.85	49.04	147
	0.90	49.29	146
	0.95	49.66	145
	0.99	50.50	143
vp_2	0.55	36.33	198
	0.60	36.37	198
	0.65	36.43	198
	0.70	36.53	197
	0.75	36.65	196
	0.80	36.80	196
	0.85	36.98	195
	0.90	37.21	194
	0.95	37.54	192
	0.99	38.28	188
vp_3	0.55	32.41	222
	0.60	32.44	222
	0.65	32.49	222
	0.70	32.58	221
	0.75	32.69	220
	0.80	32.82	219
	0.85	32.99	218
	0.90	33.19	217
	0.95	33.48	215
	0.99	34.09	211

5.2.2 *Travel time and throughput performance of the elevator*

Expected (single- and dual-) cycle times and throughput capacities of the elevators lifting table for the selected double-deep SBS/RS, which are presented in the Table 5, are given on the basis of the performed analysis.

Table 5. Expected cycle time and throughput performance of the elevators lifting table.

		Expected cycle time of the elevators lifting table		Throughput performance of the elevators lifting table	
Elevators configuration	Velocity profile vp_i	$E(\mathrm{SCC})_{\mathrm{LIFT}}$	$E(\mathrm{DCC})_{\mathrm{LIFT}}$	$\lambda(\mathrm{SCC})_{\mathrm{LIFT1}}$	$\lambda(\mathrm{DCC})_{\mathrm{LIFT1}}$
Config. 1	vp_1	8.91	14.17	404	508
	vp_2	8.47	13.62	425	529
	vp_3	7.68	12.53	469	575
		$E(\mathrm{SCC})_{\mathrm{LIFT}}$	$E(\mathrm{DCC})_{\mathrm{LIFT}}$	$\lambda(\mathrm{SCC})_{\mathrm{LIFT2}}$	$\lambda(\mathrm{DCC})_{\mathrm{LIFT2}}$
	vp_1	8.91	/	808	/
Config. 2	vp_2	8.47	/	850	/
	vp_3	7.68	/	938	/
		$E(\mathrm{SCC})_{\mathrm{LIFT}}$	$E(\mathrm{DCC})_{\mathrm{LIFT}}$	$\lambda(\mathrm{SCC})_{\mathrm{LIFT2}}$	$\lambda(\mathrm{DCC})_{\mathrm{LIFT2}}$
	vp_1	/	14.17	/	1016
Config. 3	vp_2	/	13.62	/	1057
	vp_3	/	12.53	/	1149

Notes: Config. 1 deals for the elevator with one lifting table only, which is operating on the basis of single or double transactions. Config. 2 deals for the elevator with two lifting tables operating on the basis of single transactions, only. Config. 3 deals for the elevator with two lifting tables operating on the basis of double transactions, only.

Expected (single- and dual-) cycle times and consequently the throughput performance of the elevator depend on the selected SBS/RS, elevators configuration (Config. 1, 2 or 3) and the velocity profile vp_i of the elevators lifting table (v_y and a_y). Because the elevator is usually a bottleneck in the SBS/RS, it will operate most of the time with 100% efficiency. The fastest transactions belong to the elevators lifting table with relatively high velocity (vp_3) for all three configurations. The opposite, the slowest transactions belong to the elevators lifting table with low velocity (vp_1) for all three configurations.

Generally, the expected cycle time is smaller when the vertical velocity v_y is increased. The exceptions could be SBS/RS, where the number of tiers M is relatively low (small SBS/RS). In this case, majority of the transactions will be relatively short, which has a consequence that the maximum velocity of the elevators lifting table will never be reached. This proves that we have to be extremely careful when we are selecting the right velocity profile for the elevators lifting table (it is not always true that high velocity profile is better for the throughput performance).

According to the elevators configuration, the highest throughput capacity belongs to the Config. 3, with the installation of two lifting tables that can operate independent of each other on the double command mode.

5.2.3 *Throughput performance of the SBS/RS*

Table 6 summarises expected dual-command cycle times of the elevators lifting table $E(DCC)_{LIFT}$ and the shuttle carrier $E(DCC)_{SCAR}$, the throughput performance of the elevators lifting table $\lambda(DCC)_{LIFT}$ and the shuttle carrier $\lambda(DCC)_{SCAR}$, the efficiency of the elevator η_{LIFT} and the shuttle carrier η_{SCAR} and the throughput performance $\lambda(DCC)_{SBS/RS}$ of the SBS/RS as a whole.[3]

Table 6. Expected cycle time and throughput performance of the SBS/RS.

α	$E(DCC)_{SCAR}$(s)	$E(DCC)_{LIFT}$ (s)	$\lambda(DCC)_{SCAR}$ (totes/h)	$\lambda(DCC)_{SCAR}$* (totes/h)	$\lambda(DCC)_{LIFT}$ (totes/h)	η_{LIFT}	η_{SCAR}	ψ	$\lambda(DCC)_{SBS/RS}$ (totes/h)
0.55	48.33	12.53	149	1788	1149	1.00	0.64	lift	1149
0.60	48.37		149	1788		1.00	0.64	lift	
0.65	48.45		149	1788		1.00	0.64	lift	
0.70	48.55		148	1776		1.00	0.65	lift	
0.75	48.69		148	1776		1.00	0.65	lift	
0.80	48.85		147	1764		1.00	0.65	lift	
0.85	49.04		147	1764		1.00	0.65	lift	
0.90	49.29		146	1752		1.00	0.66	lift	
0.95	49.66		145	1740		1.00	0.66	lift	
0.99	50.50		143	1716		1.00	0.67	lift	
0.55	36.33	12.53	198	2376	1149	1.00	0.48	lift	1149
0.60	36.37		198	2376		1.00	0.48	lift	
0.65	36.43		198	2376		1.00	0.48	lift	
0.70	36.53		197	2364		1.00	0.49	lift	
0.75	36.65		196	2352		1.00	0.49	lift	
0.80	36.80		196	2352		1.00	0.49	lift	
0.85	36.98		195	2340		1.00	0.49	lift	
0.90	37.21		193	2316		1.00	0.50	lift	
0.95	37.54		192	2304		1.00	0.50	lift	
0.99	38.28		188	2256		1.00	0.51	lift	
0.55	32.41	12.53	222	2664	1149	1.00	0.43	lift	1149
0.60	32.44		222	2664		1.00	0.43	lift	
0.65	32.49		222	2664		1.00	0.43	lift	
0.70	32.58		221	2652		1.00	0.43	lift	
0.75	32.69		220	2640		1.00	0.44	lift	
0.80	32.82		219	2628		1.00	0.44	lift	
0.85	32.99		218	2616		1.00	0.44	lift	
0.90	33.19		217	2604		1.00	0.44	lift	
0.95	33.48		215	2580		1.00	0.45	lift	
0.99	34.09		211	2532		1.00	0.45	lift	

Notes: $\lambda(DCC)_{SCAR}^* = \lambda(DCC)_{SCAR}M$. For the shuttle carrier: the upper part of the Table 6 stands for the velocity profile vp_1, the middle part of the Table 6 stands for the velocity profile vp_2 and the lower part of the Table 6 stands for the velocity profile vp_3. For the elevators lifting table: all three parts of the Table 6 stand for the velocity profile vp_3.

Because of the SBS/RS is composed of the elevator and the tier-captive shuttle carriers that are working in each tier of the SBS/RS, the possible bottleneck is required to be found for calculating the SBS/RS performance as a whole.

The efficiency η of the elevator and the shuttle carrier is calculated by Equation (49):

$$\eta = \frac{\min\left(\lambda(\mathrm{DCC})_{\mathrm{SCAR}}, \lambda(\mathrm{DCC})_{\mathrm{LIFT}}\right)}{\max\left(\lambda(\mathrm{DCC})_{\mathrm{SCAR}}, \lambda(\mathrm{DCC})_{\mathrm{LIFT}}\right)} \tag{49}$$

The expected bottleneck ψ is calculated by Equation (50):

$$\psi = \max\left(\lambda(\mathrm{DCC})_{\mathrm{SCAR}}, \lambda(\mathrm{DCC})_{\mathrm{LIFT}}\right) \tag{50}$$

The SBS/RS system performance $\lambda(\mathrm{DCC})_{\mathrm{SBS/RS}}$ as a whole is calculated by Equation (51):

$$\lambda(\mathrm{DCC})_{\mathrm{SBS/RS}} = \min\left(\lambda(\mathrm{DCC})_{\mathrm{SCAR}}, \lambda(\mathrm{DCC})_{\mathrm{LIFT}}\right) \tag{51}$$

Because the elevator (elevators lifting table) is usually a bottleneck in the SBS/RS (Table 6), shuttle carriers work with relatively small utilisation depending on the vp_i and λ for the selected SBS/RS.

The throughput performance λ of the SBS/RS is calculated according to the expected bottleneck of the elevator (elevators lifting table) or the shuttle carrier. Usually, the bottleneck of the SBS/RS is the elevator and in relatively small cases, a shuttle carrier (in case of small number of tiers and large numbers of columns). Throughput performance of the SBS/RS $\lambda(\mathrm{DCC})_{\mathrm{SBS/RS}}$ as a whole depends mostly on the throughput performance of the elevator $\lambda(\mathrm{DCC})_{\mathrm{LIFT}}$.

Generally, when selecting a shuttle carrier, velocity profile vp_i provides significant information on calculating the shuttle carrier's efficiency. For example, if we have a SBS/RS with $\lambda = 0.95$ and vp_3, the throughput capacity of the elevator would be $\lambda(\mathrm{DCC})_{\mathrm{LIFT}} = 1149$ totes per hour, meanwhile the throughput capacity of all shuttle carriers would be $\lambda(\mathrm{DCC})_{\mathrm{SCAR}} = 2581$ totes/hour. According to the extremly high throughput capacity $\lambda(\mathrm{DCC})_{\mathrm{SCAR}}$ of shuttle carriers, the assumption that in each tier there is a single shuttle carrier could be released.

6. Conclusion

In this paper, the analytical travel time model for double-deep SBS/RS is presented. In the proposed model, the real operating characteristics of the elevators lifting table and the shuttle carrier along with the FEM 9.851 guideline have been used. In the proposed model, it is assumed that the rearrangement during the storage process does not occur, meanwhile in case of retrieval process the access to the second lane of the SBS/RS might be blocked by the blocking tote in the first lane. The latter can be solved by rearranging the blocking tote to the nearest free storage location. Therefore, considering the randomised storage assignment rule and the above mentioned conditions, the proposed analytical travel time model for double- deep SBS/RS has been developed.

The proposed model presents an efficient tool for evaluating the system (throughput) performance of the double-deep SBS/RS, which is manly influenced by the following decision variables: M, A, C, v_y, a_y, v_x, a_x, α.

Generally, the best performance is achieved using efficient (fast) drives for both elevators lifting tables and shuttle carriers. Since the elevator works most of the time with the efficiency $\eta = 1.00$ (see Table 6), the system performance will greatly depend on the elevators performance. On the contrary, the efficiency of the shuttle carriers range from $\eta = 0.43$ to $\eta = 0.67$, therefore the assumption that in each tier there is a single shuttle carrier could be released (the application of non tier-captive configuration).

The proposed model proves to be useful when designing double-deep SBS/RS and could help the warehouse designer to analyse the efficiency of SR layout along with the kinematic properties of the SBS/RS in the early stage of project.

For the future work, some special designs of shuttle carriers which can receive more totes at a time (shuttle carriers with more load attachments), should be analysed. Since the elevator is always the bottleneck of the SBS/RS, the application of multi-shuttle elevators lifting table, should be analysed as well.

Disclosure statement

No potential conflict of interest was reported by the author.

Notes

1. For a detailed representation of the above mentioned conditions, see papers from Lerher et al. (2005) and Hwang and Lee (1990).

2. For a detailed representation of the above mentioned conditions, see papers from Lerher et al. (2005) and Hwang and Lee (1990).
3. Since the elevator Config. 3 proves to be the most efficient, the expected dual-command cycle times and the throughput capacity of Config 3. with the velocity profile vp_3 (Table 5), have been used.

References

Bekker, J. 2013. "Multi-objective Buffer Space Allocation with the Cross-entropy Method." *International Journal of Simulation Modelling* 12 (1): 50–61.

Carlo, H. J., and I. F. A. Vis. 2012. "Sequencing Dynamic Storage Systems with Multiple Lifts and Shuttles." *International Journal of Production Economics* 140 (2): 844–853.

De Koster, M. B. M., T. Le-Duc, and Y. Yu. 2008. "Optimal Storage Rack Design for a 3-Dimensional Compact AS/RS." *International Journal of Production Research* 46 (6): 1495–1514.

FEM 9.851. 1978. "Leistungsnachweis Für Regalbediengeräte Spielzeiten [Performance Data of Storage and Retrieval Machines: Cycle Times]." *European Federation of Materials Handling*.

Hwang, H., and S. B. Lee. 1990. "Travel-time Models Considering the Operating Characteristics of the Storage and Retrieval Machine." *International Journal of Production Research* 28 (10): 1779–1789.

Lerher, T. 2013. "Modern Automation in Warehousing by Using the Shuttle Based Technology." In *Automation Systems of the 21st Century: New Technologies, Applications and Impacts on the Environment & Industrial Processes*, edited by Doug Arent and Monica Freebush, 51–86. New York: Nova Science.

Lerher, T., M. Sraml, J. Kramberger, I. Potrc, M. Borovinsek, and B. Zmazek. 2005. "Analytical Travel Time Models for Multi Aisle Automated Storage and Retrieval Systems." *The International Journal of Advanced Manufacturing Technology* 30 (3–4): 340–356.

Lerher, T., I. Potrc, M. Sraml, and T. Tollazzi. 2010. "Travel time Models for Automated Warehouses with Aisle Transferring Storage and Retrieval Machine." *European Journal of Operational Research* 205 (3): 571–583.

Lerher, T., M. Sraml, I. Potrc, and T. Tollazzi. 2010. "Travel Time Models for Double-deep Automated Storage and Retrieval Systems." *International Journal of Production Research* 48 (11): 3151–3172.

Lerher, T., B. Y. Ekren, G. Dukic, and B. Rosi. 2015a. "Travel Time Model for Shuttle-based Storage and Retrieval Systems." *The International Journal of Advanced Manufacturing Technology* 78 (9–12): 1705–1725.

Lerher, T., B. Y. Ekren, Z. Sari, and B. Rosi. 2015b. "Simulation Analysis of Shuttle Based Storage and Retrieval Systems." *International Journal of Simulation Modelling* 14 (1): 48–59.

Marchet, G., M. Melacini, S. Perotti, and E. Tappia. 2013. "Development of a Framework for the Design of Autonomous Vehicle Storage and Retrieval Systems." *International Journal of Production Research* 51 (14): 4365–4387.

Oser, J., and P. Garlock. 1998. "Technology and Throughput of Double-deep Multi-shuttle aS/RS." In *Progress in Material Handling Research*, edited by R. J. Graves, et al., 409–423. Charlotte, NC: Material Handling Institute.

Oser, J., and M. Ritonja. 2004. "Expected Cycle Time in a Class-based Single- and Double-deep Storage System." In *Progress in Material Handling Research*, edited by R. Meller, et al., 310–325. Charlotte, NC: Material Handling Institute.

Ritonja, M. 2003. "Spielzeitberechnung Von Bedienstrategien Von Regalbediengäreten Mit Mehrfach-Lastaufnahmemitteln [Traveltime Calculation of Operating Strategies of Storage and Retrieval Machines with Multiple Load Handling Devices]." PhD diss., Graz University of Technology.

Sari, Z., C. Saygin, and N. Ghouali. 2005. "Travel-time Models for Flow-rack Automated Storage and Retrieval Systems." *The International Journal of Advanced Manufacturing Technology* 25 (9–10): 979–987.

Sari, Z., L. Ghomri, B. Y. Ekren, and T. Lerher. 2014. "Experimental Validation of Travel Time Models for Shuttle-based Automated Storage and Retrieval System." Paper presented at the International Material Handling Research Colloquium, Cincinnati, June 23–27.

Smew, W., P. Young, and J. Geraghty. 2013. "Supply Chain Analysis Using Simulation, Gaussian Process Modelling and Optimisation." *International Journal of Simulation Modelling* 12 (3): 178–189.

Xu, X., G. Shen, Y. Yu, and W. Huang. 2015. "Travel Time Analysis for the Double-deep Dual-shuttle AS/RS." *International Journal of Production Research* 53 (3): 757–773.

Yu, Y., and M. B. M. De Koster. 2009a. "Designing an Optimal Turnover-based Storage Rack for a 3D Compact Automated Storage and Retrieval System." *International Journal of Production Research* 47 (6): 1551–1571.

Yu, Y., and M. B. M. De Koster. 2009b. "Optimal Zone Boundaries for Two-class-based Compact Three-dimensional Automated Storage and Retrieval Systems." *IIE Transactions* 41 (3): 194–208.